ChemCatChem

Research Article
doi.org/10.1002/cctc.202201268

Chemistry Europe
European Chemical Societies Publishing

www.chemcatchem.org

Olefin Metathesis under Spatial Confinement and Continuous Flow: Investigation of Isomeric Side Reactions with a Grubbs–Hoveyda Type Catalyst

André Böth[+],[a] Thomas Roider[+],[a] Felix Ziegler,[b] Xiulan Xie,[a] Michael R. Buchmeiser,[b] and Ulrich Tallarek*[a]

A 2nd-generation Grubbs–Hoveyda type catalyst was immobilized inside mesoporous silica and used in the ring-closing metathesis (RCM) of an α,ω-diene to a large macro(mono)cycle. The goal was to investigate the relationship between substrate concentration, reaction time, and overall experiment time on the rate of isomerization under spatial (mesopore space) confinement with continuous-flow microreactors. RCM reactions are commonly monitored by ^{1}H NMR analysis, however, elucidation of reaction mixtures yielding large rings with a difference of only a single carbon atom remains difficult, because NMR signals are sometimes indistinguishable. In this work, an analytical platform with on-line separation and detection of UV-active substrate as well as (side) products by high-performance liquid chromatography and a UV/Vis-diode array detector (DAD) plus mass spectrometry served as enabling technology to quantify yield and selectivity under the respective reaction conditions. Using this setup, competitive reaction equilibria and isomerization reactions, in particular, could be resolved. Identification and quantification of relevant compounds of the reaction scheme under spatial confinement became possible despite chemical similarity. Kinetic data revealed that isomerization increases with higher substrate concentrations (up to 250 mM) and longer reaction times (from 1.2 to 18.6 min), but shows a distinct decline for prolonged overall experiment times (up to ~250 min).

Introduction

Ruthenium-based olefin metathesis catalysts are compelling tools to generate new carbon-carbon double bonds.[1–4] However, the 2nd-generation Grubbs catalyst[5] and its phosphine-free analogue, the 2nd-generation Grubbs–Hoveyda catalyst,[6] known for their outstanding versatility, are prone to ruthenium-hydride formation and thus to double-bond isomerization.[7] As a result, a wider range of side products and macro(mono)cycles (MMCs) of different ring sizes can be observed, which negatively impacts product yield and selectivity. It has further been proposed that intrinsic catalyst deactivation and formation of isomeric species are connected.[8] Consequently, the combined identification and quantification of relevant isomeric compounds provides deeper insight into the relationship between double-bond isomerization and catalyst deactivation. Due to its impact on selectivity, this issue moves into the focus of our work in the particular context of olefin metathesis under spatial confinement.

In addition, the separation of such complex reaction mixtures often cannot be accomplished with standard purification techniques.[9] It is then common to study reaction mixtures by ^{1}H NMR and to determine conversion and selectivity from the NMR data. However, the interpretation of reaction mixtures with a large α,ω-diene as starting material remains challenging, because the signals of the product and the side products as well as the α,ω-diene may become indistinguishable.[10] Alternatively, gas chromatographic methods have been established to determine the progress of RCM reactions.[11] Still, involatile compounds like oligomers complicate the quantification procedure and require indirect measurement based on calibration to indicate conversion of the substrate and formation of RCM (by-)products.

The major research theme underlying this work is catalysis under confinement, i.e., how the spatial confinement engendered by the pore system inside mesoporous supports can be used to direct and tune especially the selectivity of a catalytic process. Here, we investigate olefin metathesis and macrocyclization selectivity, in particular. In previous work, we have studied RCM reactions to identify suitable mesoporous supports, establish a route to pore-selective immobilization of catalysts, and identify and understand confinement effects with the chosen catalysts.[12–14] It was shown that catalytic reactions

[a] A. Böth,[+] T. Roider,[+] Dr. X. Xie, Prof. U. Tallarek
Department of Chemistry
Philipps-Universität Marburg
Hans-Meerwein-Strasse 4
D-35032 Marburg (Germany)
E-mail: tallarek@staff.uni-marburg.de
Homepage: http://www.uni-marburg.de/fb15/ag-tallarek
[b] Dr. F. Ziegler, Prof. M. R. Buchmeiser
Institute of Polymer Chemistry
Universität Stuttgart
Pfaffenwaldring 55
D-70569 Stuttgart (Germany)
[+] These authors contributed equally to this work.

Supporting information for this article is available on the WWW under https://doi.org/10.1002/cctc.202201268

and competitive equilibria establish on a timescale of seconds up to a few minutes, requesting a continuous-flow microreactor system for kinetic studies rather than batch operation, combined with a powerful, on-line coupled multidimensional analytical platform (high-resolution separation and detection) for the elucidation of reaction mechanisms.

To meet these conditions, the 2nd-generation Grubbs–Hoveyda type catalyst $RuCl_2$(*N*-mesityl-*N*-(3-(trimethoxysilyl)prop-1-yl)-imidazol-2-ylidene)(CH-2-(2-PrO-C_6H_4)) was selectively immobilized inside mesoporous silica particles[13] and continuous-flow operation was subsequently realized using a high-end HPLC configuration equipped with a packed microreactor containing the modified silica particles.[12] This setup allowed fully automatic and precise adjustments of temperature and flow rate, in contrast to the often used syringe-pump design. As a drawback, that previous work only utilized a fraction collector to collect the effluent from the column, remove the solvent under reduced pressure, and analyze the residue offline via ^{1}H NMR. It should be noted that the substrates employed before were all UV-inactive.

Due to the problems with offline ^{1}H NMR analysis of RCM reaction mixtures and the detection of UV-inactive substrates and (side) products, we improved this setup in the present work by adapting a UV-active substrate and coupling a second dimension on-line, including a chromatographic column (for high-resolution chemical separations), a UV/Vis-DAD, and electrospray ionization-mass spectrometry (ESI-MS). Combination of the first (microreactor) dimension with the second (separation-analysis) dimension enabled real-time reaction control (monitoring) and simultaneous quantification of relevant compounds. In this regard, ESI-MS is important to receive an overview of the formed by-products. The 2D-LC/MS setup is particularly suited for complex reaction mixtures, e.g., from RCM reactions that yield large rings, where target molecules are nearly identical and, as a result, need to be chromatographically separated prior to analysis in order to reliably determine yield and selectivity. We adapted this enabling technology to study in-depth isomeric side reactions during olefin metathesis under spatial confinement. These side reactions are an integral part of the total reaction scheme and important to address when resolving the impact of the confinement on selectivity and, for that purpose, screening substrate concentration, reaction time, and temperature. In particular, we could show which by-products are formed (and when), resolved distinct performance stages of the microreactors characterized by different selectivities, and indicated the relationship with concomitant catalyst deactivation. This insight would not have become available with batch reactor operation and/or by using offline ^{1}H NMR analysis. Complementarily, by scaling up to a semi-preparative column and exchanging ESI-MS with a fraction collector, offline analysis became possible, which we used to investigate the dependence of the isomerization rate on substrate concentration and overall experiment time.

Figure 1 presents an overview of the investigated reaction (Figure 1a), common by-products from isomerization (Figure 1b), and the used catalyst (Figure 1c). Problems that arise in the determination of conversion and selectivity for the reaction mixture via ^{1}H NMR analysis from overlapping signals are illustrated in the Supporting Information (Chapter S4) for this particular example.

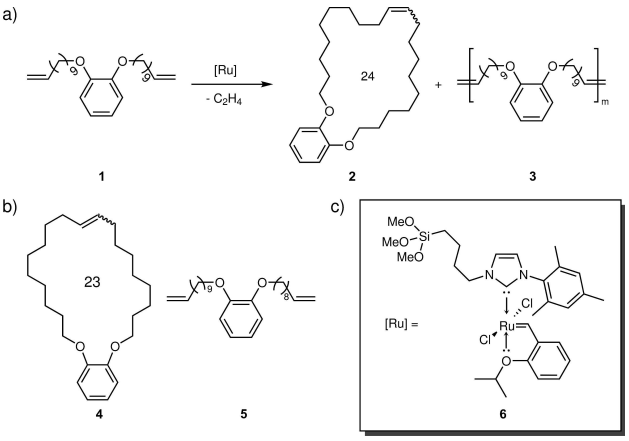

Figure 1. a) Investigated RCM reaction. b) Species formed from isomers. c) Structure of the 2nd-generation Grubbs–Hoveyda type catalyst. The trimethoxysilyl tether at the NHC serves for the covalent attachment to the internal surface of the mesoporous silica particles.

Results and Discussion

Catalyst immobilization

As in our previous work, we used spherical-shaped, mesoporous amorphous silica particles with a particle diameter of about 5 μm (mode) and a mean mesopore size of 5.9 nm.[12] Immobilization of the 2nd-generation Grubbs–Hoveyda type catalyst **6** (Figure 1c) selectively inside the mesoporous silica particles was carried out following an established protocol.[13] The particles had a specific surface area of 793 $m^2 g^{-1}$ (nitrogen physisorption) and showed a loading with **6** of 7.2 $\mu mol\, g^{-1}$ (ICP-OES).[12]

The silica particles are indeed well suited for the study of spatial confinement effects on selectivity in olefin metathesis with the chosen substrate size and size of the expected (side) products (cf. Figure 1). This can be directly inferred from the accessible porosity and effective diffusivity characteristics derived for model solutes of different size through direct (pore scale) simulations in electron tomography-based reconstructions of the particles mesopore network.[14] Obtained hindrance factor expressions quantify the extent to which transport in and through the particles is hindered compared with free diffusion in the bulk liquid. These morphology-transport relationships indicate that the pore network discriminates effectively between macro(mono)cyclization and oligomerization regarding the respective spatial requirements.

Olefin metathesis pathways

We investigated olefin metathesis pathways with the α,ω-diene **1** to the MMC product **2** and oligomer **3** (Scheme 1, cycle A),

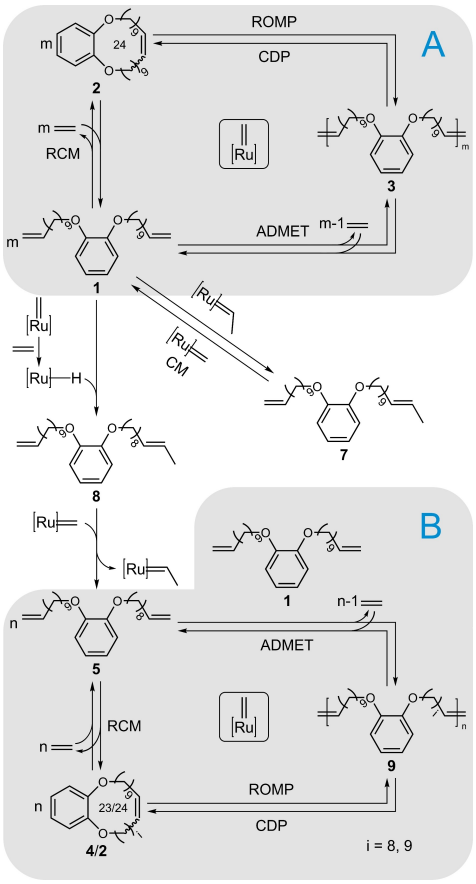

Scheme 1. Olefin metathesis pathways of the α,ω-diene **1** to the MMC **2** and oligomer **3**. Isomerization of **1** leads to a smaller substrate **5**, which is also susceptible to olefin metathesis. RCM: ring-closing metathesis, ADMET: acyclic diene metathesis, ROMP: ring-opening metathesis polymerization, CDP: cyclodepolymerization, CM: cross-metathesis. n denotes substrate equivalents and i the number of methylene groups, [Ru=] represents the metal alkylidene complex.

where we focused on individual routes resulting from isomerization of **1** followed by cross-metathesis (Scheme 1, cycle B). Because the microreactor is constantly supplied with fresh substrate solution, new ethylene is also permanently formed and affects the reaction equilibria. Also, it can be assumed that all reaction pathways including ethylene are in principle reversible.[15]

It has been proposed that ethylene decomposes the ruthenium catalyst to ruthenium hydrides, which promote isomerization.[16] A higher substrate concentration will cause a higher local ethylene concentration. Consequently, more ruthenium hydrides should be formed inside the mesoporous material and the concentration of isomers should increase. Because the focus of this work is on the formation of isomers, rather high concentrations between 25 and 250 mM were chosen for the substrate solutions. Isomerization of **1** yields **8**, whose RCM is impeded by the presence of an internal olefin (Scheme 1). After cross-metathesis of **8** to a smaller substrate **5**, however, olefin metathesis is facilitated (cycle B). Diene **5** can react with **1** or with itself by acyclic diene metathesis to form oligomer **9**, where the individual dienes of the oligomer have different chain lengths (i = 8 or 9). Backbiting of these oligomers yields either the RCM product **2** of cycle A or the RCM product **4** of substrate **5** (cycle B). Cross-metathesis of substrate **1** also leads to a non-terminal alkene **7**.

Experimental configuration and 2D-LC/MS setup

Olefin metathesis of substrate **1** with the immobilized Grubbs–Hoveyda type catalyst **6** under continuous-flow was realized by adapting the 2D-LC/MS configuration illustrated in Figure 2. In the first dimension of that setup, a binary pump (4) was used to feed reactant solution into a microreactor column packed with the modified silica particles (4.6 mm inner diameter × 15 mm effective packed-bed length; packed-reactor volume, $V_{reactor}$ ≈ 0.18 mL) at a precisely set and constant flow rate. The residence time of the substrate solution on the packed microreactor (and thus, the reaction time) was controlled by the pump flow rate and depended on the volume in the microreactor available to the pumped solution. The microreactor was located in a temperature-controlled column oven compartment (9), which also allowed the reaction temperature to be adjusted within the system. Behind the reactor, there was an injection valve (5) connecting the first with the second dimension that allowed to analyze the reaction solution (effluent). In the second (analytical) dimension, the injected sample was then purified by a chromatographic column (8) and the separated compounds were detected using an on-line DAD (7) and ESI-MS (12). Through the replacement of the analytical-scale chromatographic column by a semi-preparative column and ESI-MS by a fraction collector (11), additional offline analysis was possible. A more detailed description of all individual components of the 2D-LC/MS setup can be found in the Supporting Information (Chapter S2, Figure S1).

To identify all reactants, products, and side products and to quantify their concentrations with the 2D-LC/MS system, it is necessary to identify conditions for which all compounds were baseline-separated by the chromatographic column of the second dimension (8). For that purpose, a batch reaction of **1** with the modified silica material was carried out to generate a sample that was subsequently used to determine optimal separation conditions. Figure 3 shows an example chromatogram, in which the dienes as well as the MMCs and oligomers are apparent.

Because the HPLC separation had to be completely finished after each injection of sample onto the chromatographic column before the next injection can take place, it was necessary to keep the time for the analysis cycle as short as possible. Especially when the lifetime of the microreactor is limited due to catalyst deactivation, a short analysis time is essential to be able to generate a sufficient number of data points for, e.g., different substrate concentrations, reaction times, and temperatures with each microreactor. The α,ω-diene **1**, RCM products **2** and **4**, as well as the isomeric species **5** and **7** (Scheme 1) could be eluted from the column and separated

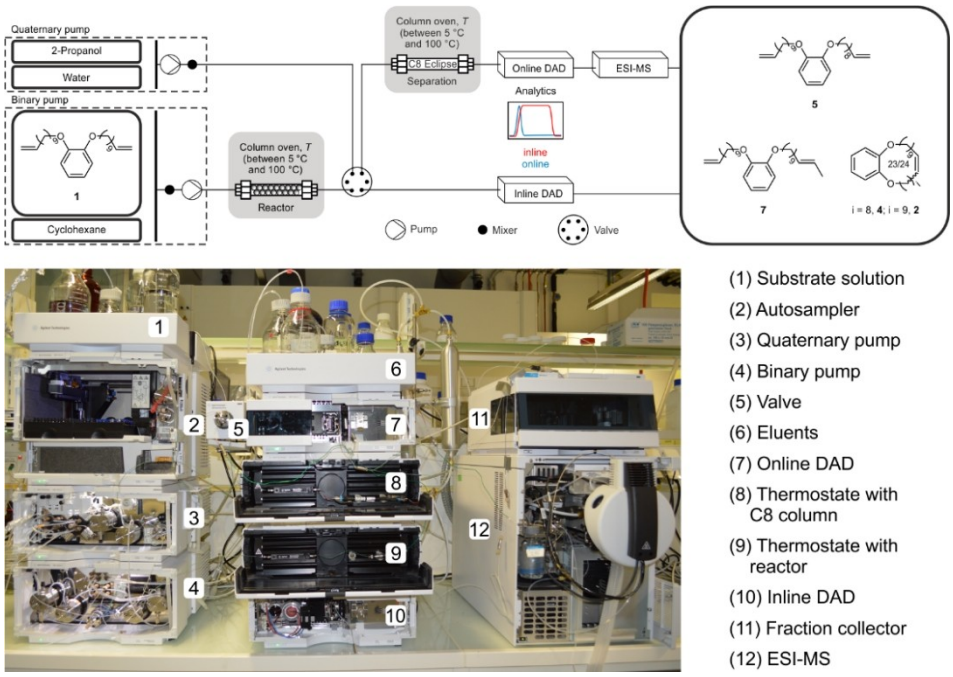

Figure 2. Photograph illustrating the two-dimensional continuous-flow platform adapted for the screening of olefin metathesis under spatial confinement using substrate **1** (25, 50, 100, and 250 mM in absolute cyclohexane, (1)). An injection valve (5), located behind the microreactor compartment (9), connects the first (reaction) dimension with the second (analytical) dimension that enables the high-resolution chromatographic separation of the reaction mixture (8) and on-line analysis of the separated compounds using a DAD (7) and ESI-MS (12). Steady-state operation of the microreactor was confirmed by an in-line DAD (10).

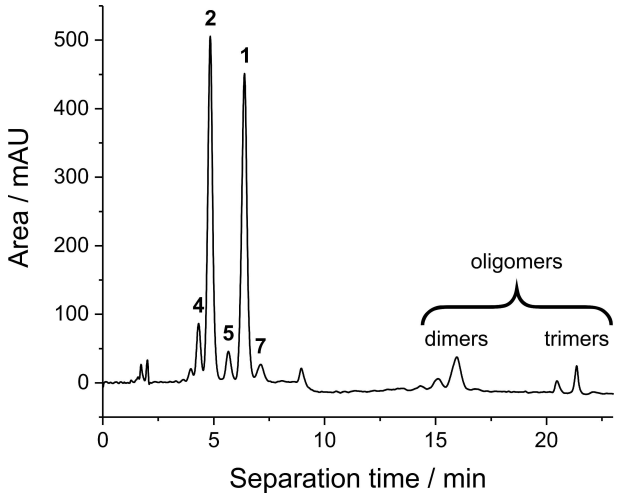

Figure 3. Separation of a RCM reaction sample of substrate **1** by reversed-phase liquid chromatography on an analytical-scale HPLC column packed with 5 μm-sized, C8-modified silica particles (detection at 208 nm).

under isocratic conditions, that is, with a constant composition of the eluent, in less than eight minutes (Figure 3).

For the oligomers, however, it was necessary to run a gradient in the eluent composition to elute them in a timely manner, which resulted in an overall duration of the chromatographic separation of about 23 minutes. Moreover, after applying the mobile phase gradient, equilibration of the separation column was needed before the next injection, which added another ~3 minutes. Due to these circumstances, we did not further investigate the oligomers, which allowed us to shorten the separation time and focus only on the isomeric compounds. Details of the separation conditions used for the screenings and further information on the calibration of relevant compounds can be found in the Supporting Information (Chapters S2 and S3, Figures S2–S6).

The process adapted for the slurry-packing of the stainless-steel microreactor columns with the selectively modified silica particles has been described in detail before.[12] The packing station for the microreactors illustrated in Figure 4 guaranteed the preparation of dense and stable as well as homogeneous beds of these fine (~5 μm-sized) catalyst particles. This also ensured that relatively little solute dispersion occurs during hydrodynamic flow and transport of substrate solution in a continuous-flow experiment[17] and that plug-flow conditions were realized on the microreactors.[18] These conditions allow the transformation of flow rate through a reactor (and mean residence time on a reactor) into a sharp reaction time of the transported substrate molecules.[19] Consequently, a high-resolution reaction time control and discrete variation of reaction times was realized by straight adjustment and programming of the volumetric flow rate delivered by the high-precision, high-pressure pumps.[20]

For olefin metathesis under continuous-flow conditions substrate solution was continuously flushed through the microreactor at a set volumetric flow rate Q using a binary pump. Additionally, the temperature was set to $T = 50\,^{\circ}C$ and held

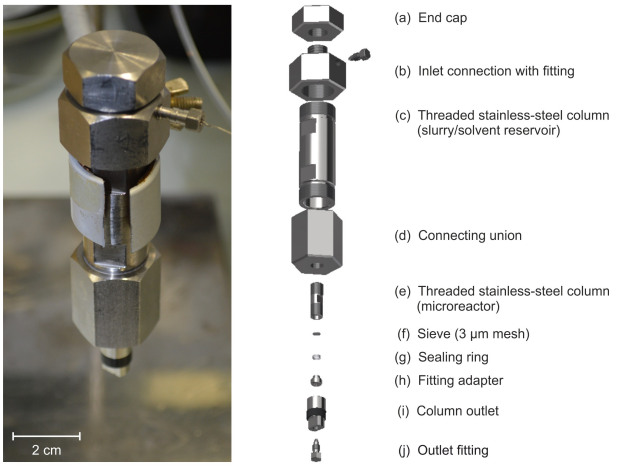

Figure 4. Setup used for the slurry-packing of microreactor columns (left) and its individual components (right). The packing station was connected via inlet (b) to a binary pump of the HPLC equipment.

constant by the column oven. Translating flow rate into reaction time on the reactor was accomplished by measuring the mean residence time ($\bar{t}_{res}$) of the substrate on a catalytically inactive microreactor.[12] Because **1** was partially size-excluded from the mesopores of the particles[14] and was also retained on the column through adsorption with the carbonyl oxygen onto the residual silanol groups of the silica surface,[13] we recorded mean residence times of **1** (which represent the effects of size-exclusion and adsorption) to express reaction times for the substrate solutions in contact with a packed microreactor. These $\bar{t}_{res}$(**1**) were determined via concentration profiles of **1** recorded from pulse injections onto the microreactor after the experiments, when the catalyst was mostly inactive. Flow rates used in the experiments and corresponding reaction times are summarized in Table 1.

HPLC yield and selectivity

HPLC yield and selectivity for the MMC product and the isomers were determined as follows (Eqs. 1–3):

$$\text{HPLC yield (MMC)} = \frac{n(\text{MMC})}{n_0(\text{Substrate})} \quad (1)$$

$$\text{HPLC yield (Isomers)} = \frac{n(\text{Isomers})}{n_0(\text{Substrate})} \quad (2)$$

$$\text{Selectivity} = \frac{n(\text{MMC})}{n(\text{MMC}) + n(\text{Isomers})} \quad (3)$$

Table 1. Reaction times of substrate **1** on microreactors packed with the silica particles containing the 2nd-generation Grubbs–Hoveyda type catalyst **6**.

Flow rate Q [mL min^{-1}]	Reaction time t_{rct} [min]
0.01	18.6
0.02	9.3
0.04	4.4
0.06	3.1
0.1	1.9
0.14	1.2

We first investigated how different reaction times affect reaction and isomerization. For this purpose, a substrate concentration of 25 mM was selected and flow rates were varied from 0.02 to 0.14 mL min^{-1}, starting with the lowest flow rate (Table 1). The results of this screening are shown in Figure 5. During the overall experiment time of ~250 minutes, no isomeric compounds could be detected. For the isomerization process to occur, the active catalyst needs to react with ethylene to form the ruthenium hydride species.[16] For the selected reaction conditions it can be assumed that the yield (and the resulting ethylene concentration) was insufficient to produce a significant amount of ruthenium hydrides. In addition, using higher flow rates ensures that the produced ethylene can be removed more efficiently from the microreactor, hindering the isomerization process. The general decrease in yield with increasing experiment time in Figure 5 is attributed to catalyst deactivation.[16]

As a consequence, for subsequent experiments we selected the lowest possible flow rate (0.01 mL min^{-1}, limited by the pump), translating to the longest reaction time (Table 1), to favor isomer formation, and increased substrate concentration substantially (up to 250 mM) to push ethylene production in the microreactor and favor isomerization further. The results of these experiments are summarized in Figure 6.

The grey-shaded areas in Figure 6 indicate the different substrate concentrations used for that screening (25 mM→250 mM→50 mM). Times between these areas were needed for

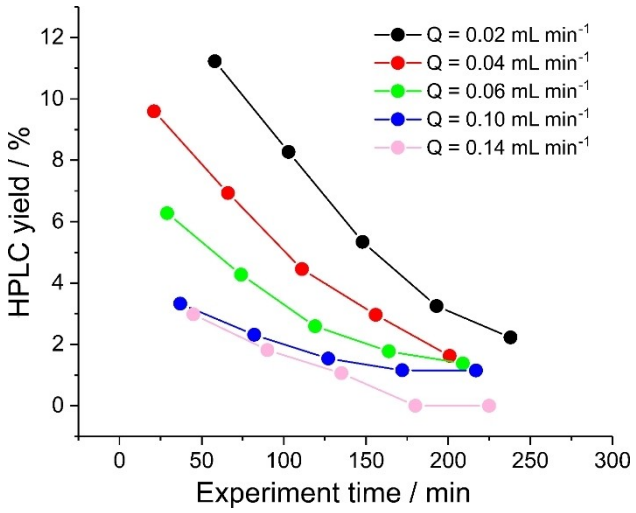

Figure 5. Reaction of substrate **1** with the immobilized 2nd-generation Grubbs–Hoveyda type catalyst **6**. **1** was supplied at different flow rates (Q = 0.02–0.14 mL min^{-1} varied automatically from low to high), corresponding to the reaction times listed in Table 1 (substrate concentration: 25 mM, T = 50 °C). HPLC yield of MMC **2** was calculated according to Eq. (1).

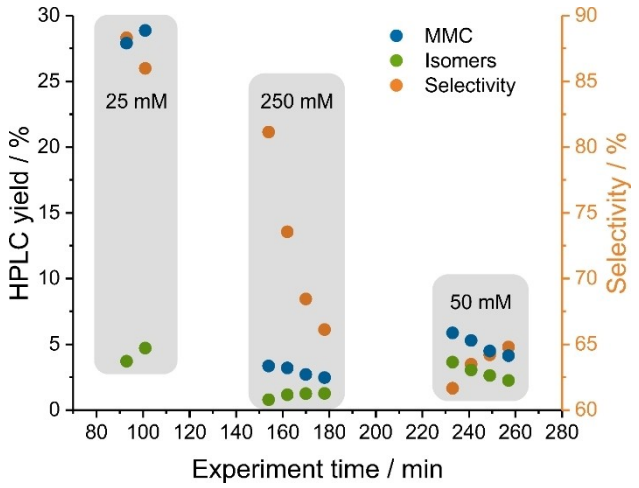

Figure 6. HPLC yield and selectivity in the RCM of substrate **1** to MMC **2** and isomers **5** and **7** calculated according to Eqs. (1)–(3). **1** was supplied at different concentrations (indicated in the figure), but with a constant flow rate Q of 0.01 mL min^{-1}, corresponding to a reaction time of 18.6 minutes (T = 50 °C).

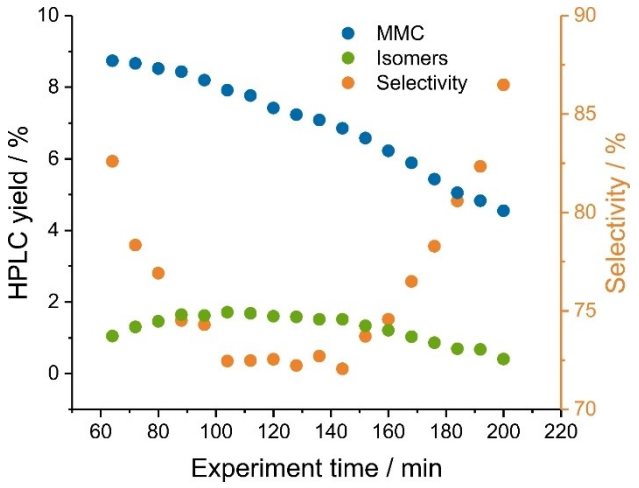

Figure 7. HPLC yield and selectivity in the RCM of substrate **1** to MMC **2** and the isomers **4**, **5**, and **7** calculated using Eqs. (1)–(3). **1** was supplied at a constant flow rate Q of 0.01 mL min^{-1}, corresponding to a reaction time of 18.6 minutes (substrate concentration: 100 mM, T = 50 °C).

the reactor to equilibrate at the new concentrations. During these times, catalyst deactivation nevertheless progressed. Already with a substrate concentration of 25 mM, isomeric compounds started to form (i.e., between 80 and 110 minutes in Figure 6). This can be attributed to the relatively high yield (~30 %) compared to the previous reactor and the generation of a sufficient amount of ethylene to form the ruthenium hydride species. With a concentration of 250 mM the amount of isomers increased even further and a sudden drop of selectivity (until a minimum of ~65 %) could be measured. Interestingly, with a concentration of 50 mM, the selectivity started to increase again. We assume that the reason for this increase in selectivity is more likely the prolonged experiment time (~250 min) than the change in concentration.

To verify this assumption, we conducted a flow experiment at the same flow rate of 0.01 mL min^{-1} (as before, Figure 6), but without changing the initial substrate concentration, which was now set to 100 mM. The results of this control experiment are summarized in Figure 7. Microreactor performance showed the same pattern as for the previous reactor (Figure 6), but with a lesser decrease in selectivity. This time, a plateau from about 100 to 140 min could be observed, followed by a sudden increase in selectivity, which reinforces the assumption that the selectivity increase (noticed in Figure 6) is based on the experiment time rather than substrate concentration.

In order for the isomerization products to be formed, ruthenium hydride species must first be generated, for which ethylene is required. Three different stages of microreactor performance can be distinguished. In the first stage (up to 100 minutes), a higher yield is present, as the catalyst is still mostly active, which also leads to the formation of a large amount of ethylene. Because of the high local ethylene concentration, the ruthenium hydride species can also form very well. Therefore, more and more isomers are generated during this stage and the selectivity decreases until it reaches a plateau at about 100 minutes. At this point, the second stage from 100 to 145 minutes begins, in which enough ethylene is formed to allow formation of new ruthenium hydride species and selectivity therefore does not change over a longer period of time. The observed plateau can be described as a steady-state between the formation and decomposition of the ruthenium hydride species. After the plateau, the third stage (140 to 200 minutes) of microreactor performance begins. In this third stage, the deactivation of the catalyst has progressed, whereby yield has decreased and thus the local concentration of ethylene is also significantly lower. As a result, the formation of additional ruthenium hydride species becomes slower than their decomposition and the selectivity begins to increase again.

The employed 2D-LC/MS setup allows to display these stages with high resolution, which on the other hand would not have been possible using ^{1}H NMR due to the overlapping signals. In addition, the combination of continuous-flow chemistry with the automated analysis of all compounds allows these measurement points to be recorded in a very short time. By contrast, in an overnight batch experiment, the presence of these different stages of microreactor performance would have been obscured, and it would be much more time-consuming to generate all points individually via batch operation. In addition, it has to be ensured then that the solutions can be well quenched at different points in order to assign reaction times sufficiently discrete.

Conclusions

We have shown that the 2D-LC/MS setup used in this work is an enabling analytical tool for elucidating reaction mechanisms of complex systems for which conventional approaches based on,

e.g., ^{1}H NMR analysis would be insufficient. The 2D-LC/MS setup allowed us to study olefin metathesis under spatial confinement with a focus on competitive reaction equilibria and isomerization reactions, in particular. We demonstrated which by-products are formed and could also detail, under which conditions these are formed preferentially. Importantly, distinct performance stages of microreactors operating with the 2nd-generation Grubbs–Hoveyda type catalyst immobilized inside mesoporous silica particles were resolved and shown to produce different selectivities with respect to RCM and isomerization. Also deactivation of the catalyst has a strong influence not only on the yield, but as well on the selectivity in olefin metathesis. These relationships highlighted by Figure 7 form a basis for further systematic, fundamental scientific studies about the influence of, e.g., substrate concentration, reaction and experiment time, temperature, mesoporous support and catalyst structure on the selectivity in catalysis under spatial confinement and thereby indicate the relative importance of the underlying competitive reaction equilibria.

Experimental

Chemicals and materials: The synthesis and immobilization of the 2nd-generation Grubbs–Hoveyda type catalyst were accomplished as described in our previous work.[12] Detailed information on chemicals used and the produced compounds can be found in the Supporting Information (Chapters S1 and S5).

Microreactor preparation: Packing of the microreactor (Figure 4) was conducted in the same manner as described previously.[12]

Microreactor operation: RCM reactions under continuous flow were performed by implementing commercially available HPLC instrumentation (1260 and 1290 Infinity II series, Agilent Technologies) as depicted in Figure 2. Substrate solution (25, 50, 100, and 250 mM of **1** in degassed, absolute cyclohexane) and degassed, absolute cyclohexane (both under nitrogen gas atmosphere) were connected to a binary pump (Figure 2, (4)) via a septum and metal capillary. Substrate solution was pumped at various flow rates (0.01–0.14 mL min^{-1}) through the microreactor placed in a thermostatted compartment ($T = 50\,^{\circ}C$, Figure 2, (9)). The reaction solution from the microreactor passed an in-line DAD (Figure 2, (10)) and was transferred by a valve (Figure 2, (5)) to the second (analytical) dimension. There, the reaction mixture was separated on a reversed-phase liquid chromatography column (Figure 2, (8)) and analyzed with an on-line DAD (Figure 2, (7)) and by ESI-MS (Figure 2, (12)).

Reaction monitoring: HPLC yield and selectivity were quantified through external calibration. For offline analysis, the effluent was collected by a fraction collector and the solvent was removed. Further information on the experimental setup and calibration is provided in the Supporting Information (Chapters S2 and S3).

Structure elucidation: For relevant compounds (diene **1**, isomers **5** and **7**, and MMCs **2** and **4**), ^{1}H and ^{13}C NMR spectra as well as 2D spectra (^{1}H–^{13}C HSQC and ^{1}H–^{1}H DQF-COSY) were recorded. These spectra and an exact signal assignment are summarized in the Supporting Information (Chapter S6).

Acknowledgements

Financial support by the Deutsche Forschungsgemeinschaft DFG (German Research Foundation, project ID 358283783 – SFB 1333/2 2022) is gratefully acknowledged. We thank Agilent Technologies (Waldbronn, Germany) for providing the HPLC equipment and Benjamin Peters (Instrumental Analytics R&D, Merck KGaA, Darmstadt, Germany) for the gift of the silica particles. Open Access funding enabled and organized by Projekt DEAL.

Conflict of Interest

The authors declare no conflict of interest.

Data Availability Statement

The data that support the findings of this study are available in the supplementary material of this article.

Keywords: heterogeneous catalysis · mesoporous materials · olefin metathesis · ruthenium · flow chemistry

[1] R. H. Grubbs, S. Chang, *Tetrahedron* **1998**, *54*, 4413–4450.
[2] K. C Nicolaou, P. G. Bulger, D. Sarlah, *Angew. Chem. Int. Ed.* **2005**, *44*, 4490–4527; *Angew. Chem.* **2005**, *117*, 4564–4601.
[3] C. Lecourt, S. Dhambri, L. Allievi, Y. Sanogo, N. Zeghbib, R. Ben Othman, M. I. Lannou, G. Sorin, J. Ardisson, *Nat. Prod. Rep.* **2018**, *35*, 105–124.
[4] R. Garcia-Fandino, M. J. Aldegunde, E. M. Codesido, L. Castedo, J. R. Granja, *J. Org. Chem.* **2005**, *70*, 8281–8290.
[5] M. Scholl, S. Ding, C. W. Lee, R. H. Grubbs, *Org. Lett.* **1999**, *1*, 953–956.
[6] a) S. Gessler, S. Randl, S. Blechert, *Tetrahedron Lett.* **2000**, *41*, 9973–9976; b) S. B. Garber, J. S. Kingsbury, B. L. Gray, A. H. Hoveyda, *J. Am. Chem. Soc.* **2000**, *122*, 8168–8179.
[7] Selected examples: a) V. I. Petkovska, T. E. Hopkins, D. H. Powell, K. B. Wagner, *Macromolecules* **2005**, *38*, 5878–5885; b) R. Ahuja, S. Kundu, A. S. Goldman, M. Brookhart, B. C. Vicente, S. L. Scott, *Chem. Commun.* **2008**, *2*, 253–255; c) A. Fürstner, O. R. Thiel, L. Ackermann, H.-J. Schanz, S. P. Nolan, *J. Org. Chem.* **2000**, *65*, 2204–2207; d) P. C. M. van Gerven, J. A. A. W. Elemans, J. W. Gerritsen, S. Speller, R. J. M. Nolte, A. E. Rowan, *Chem. Commun.* **2005**, *28*, 3535–3537; e) M. Martinez-Amezaga, C. M. L. Delpiccolo, L. Méndez, I. Dragutan, V. Dragutan, E. G. Mata, *Catalysts* **2017**, *7*, 111.
[8] J. Engel, W. Smit, M. Foscato, G. Occhipinti, K. W. Törnroos, V. R. Jensen, *J. Am. Chem. Soc.* **2017**, *139*, 16609–16619.
[9] K. C. Nicolaou, P. G. Bulger, D. Sarlah, *J. Am. Chem. Soc.* **2005**, *127*, 17160–17161.
[10] S. Monfette, A. K. Crane, J. A. Duarte Silva, G. A. Facey, E. N. dos Santos, M. H. Araujo, D. E. Fogg, *Inorg. Chim. Acta* **2010**, *363*, 481–486.
[11] Selected examples: a) S. Monfette, M. Eyholzer, D. M. Roberge, D. E. Fogg, *Chem. Eur. J.* **2010**, *16*, 11720–11725; b) A. Fürstner, O. R. Thiel, L. Ackermann, *Org. Lett.* **2001**, *3*, 449–451; c) E. Tzur, A. Ben-Asuly, C. E. Diesendruck, I. Goldberg, N. G. Lemcoff, *Angew. Chem. Int. Ed.* **2008**, *47*, 6422–6425; *Angew. Chem.* **2008**, *120*, 6522–6525.
[12] F. Ziegler, T. Roider, M. Pyschik, C. P. Haas, D. Wang, U. Tallarek, M. R. Buchmeiser, *ChemCatChem* **2021**, *13*, 2234–2241.
[13] F. Ziegler, J. Teske, I. Elser, M. Dyballa, W. Frey, H. Kraus, N. Hansen, J. Rybka, U. Tallarek, M. R. Buchmeiser, *J. Am. Chem. Soc.* **2019**, *141*, 19014–19022.
[14] U. Tallarek, J. Hochstrasser, F. Ziegler, X. Huang, C. Kübel, M. R. Buchmeiser, *ChemCatChem* **2021**, *13*, 281–292.
[15] a) S. Monfette, D. E. Fogg, *Chem. Rev.* **2009**, *109*, 3783–3816; b) A. H. Hoveyda, Z. Liu, C. Qin, T. Koengeter, Y. Mu, *Angew. Chem. Int. Ed.* **2020**, *59*, 22324–22348; *Angew. Chem.* **2020**, *132*, 22508–22532.

[16] S. H. Hong, A. G. Wenzel, T. T. Salguero, M. W. Day, R. H. Grubbs, *J. Am. Chem. Soc.* **2007**, *129*, 7961–7968.
[17] D. Enke, R. Gläser, U. Tallarek, *Chem. Ing. Tech.* **2016**, *88*, 1561–1585.
[18] a) H. S. Fogler, *Elements of Chemical Reaction Engineering*, 4th ed., Prentice Hall, Upper Saddle River, N. J., **2006**, Chapter 14.4.1; b) R. L. Hartman, J. P. McMullen, K. F. Jensen, *Angew. Chem. Int. Ed.* **2011**, *50*, 7502–7519; *Angew. Chem.* **2011**, *123*, 7642–7661.
[19] a) J. Yoshida, *Chem. Rec.* **2010**, *10*, 332–341; b) J. Yoshida, Y. Takahashi, A. Nagaki, *Chem. Commun.* **2013**, *49*, 9896–9904.
[20] C. P. Haas, T. Müllner, R. Kohns, D. Enke, U. Tallarek, *React. Chem. Eng.* **2017**, *2*, 498–511.

Manuscript received: October 20, 2022
Revised manuscript received: November 23, 2022
Accepted manuscript online: December 8, 2022
Version of record online: January 5, 2023